Experimental Platform for Explanted Hearts Study: Integrating Optical Mapping and Body Surface Recordings

T C Neves[1,2], V Silva[1,2], J G S Paredes[1,2], J Salinet[2], I Uzelac[1]

[1]School of Medicine, Virginia Commonwealth University, Richmond, VA, USA
[2]Federal University of ABC, São Bernardo do Campo, Brazil

Abstract

This study presents an integrated experimental platform for the electrophysiological assessment of explanted human hearts, enabling simultaneous high-resolution optical mapping with torso-mimetic body surface potential recordings. Perfused hearts are suspended in a hexagonal chamber equipped with wall-mounted electrodes mimicking body surface electrical potential measurements. This configuration allows precise temporal and spatial alignment between epicardial optical signals and model surface potentials, establishing a framework for validating non-invasive interpretations of cardiac activity.

In a representative case, rate-independent changes in conduction were observed during ventricular pacing in an explanted end-stage heart failure heart, while spontaneous tachycardia revealed variable propagation patterns. The synchronized dual-modality recordings enabled direct comparison of optical and surface signals, illustrating both the promise and the limitations of body surface potential mapping for capturing complex intramural conduction.

This approach offers a translational bridge between basic cardiac electrophysiological mechanisms and clinical diagnostics. Future enhancements will include higher electrode density and the integration of machine learning for improved electrophysiological characterization of explanted human hearts.

1. Introduction

Cardiac transplantation remains the final treatment option for patients with end-stage heart failure. Yet, the explanted diseased heart remains an underutilized resource for studying the electrical properties of advanced cardiomyopathies[1]. Direct electrophysiological analysis of failing human hearts has been limited, particularly with respect to approaches that combine high-resolution optical mapping with non-invasive techniques relevant to clinical practice.

The integration of body surface potential mapping (BSPM) with high-resolution optical mapping of explanted human hearts represents an underutilized approach in basic cardiac electrophysiology research. By implementing this novel approach at Virginia Commonwealth University (VCU Health), we are taking steps toward clinically relevant insights in translational cardiac electrophysiology. Traditional BSPM systems have often relied on indirect validation methods and animal studies to approximate human heart conditions. In contrast, our platform uses a hexagonal acrylic tank equipped with 60 electrodes for non-invasive signal acquisition and a dual-camera system with a voltage-sensitive dye to map epicardial electrical activity. This integration enhances our ability to study the human heart with both precision and clinical relevance.

By enabling detailed study of disease-specific electrophysiological alterations, the system provides a means to correlate clinical findings, such as ECG abnormalities and arrhythmia history. Its capacity to map spatiotemporal activation in failing human hearts may help to clarify conduction abnormalities manifest in BSPM signals, potentially leading to the identification of new diagnostic markers.

This study represents an initial step toward establishing a proof-of-concept platform that links research on explanted hearts with clinical electrophysiology. By presenting activation patterns on both the epicardial surface and the surrounding tank electrodes, this work illustrates how intrinsic myocardial dysfunction may manifest in BSPM-like signals. These findings offer preliminary insight into the potential for improving non-invasive arrhythmia risk stratification and informing therapeutic strategies such as ablation planning. Future iterations of the system may incorporate higher electrode density and advanced computational modeling to further refine signal interpretation and support translational applications.

2. Methods

The study team receives the explanted heart directly in the operating room immediately after its removal during cardiac transplantation, while the surgical team pro-

ceeds with implantation of the donor heart, under the approved IRB protocol. Upon retrieval, the heart is promptly rinsed with a cold cardioplegia solution (110 mM NaCl, 16 mM KCl, 10 mM NaHCO3, 16 mM MgCl2, and 1.2 mM CaCl2), which induces cardiac arrest to prevent contractions and electrical activity. This solution protects the myocardium by reducing ischemic injury and metabolic demand. In the research lab, the heart is then cannulated and positioned within a hexagonal acrylic tank using a custom 3D-printed holder that secures the aorta and stabilizes the heart for perfusion and mapping.

2.1. Heart perfusion

The heart is subjected to coronary perfusion using two custom-made cannulas inserted into the right and left coronary arteries. Perfusion is performed with a modified Tyrode solution maintained at 37 °C, composed of 120 mM NaCl, 4.7 mM KCl, 25 mM NaHCO3, 1.2 mM NaH2PO4, 1 mM MgCl2, 10 mM dextrose, and 1.8 mM CaCl2. The solution is continuously bubbled with carbogen gas (5% CO2 and 95% O2) to ensure proper oxygenation and pH stabilization.

The same solution also fills the hexagonal tank designed to mimic a patient's torso. Although the heart is fully immersed, continuous coronary perfusion must be maintained through the cannulas to provide physiologic pressure and flow conditions, typically around 30-40 ml/min.

2.2. Experimental protocol

After heart stabilization (15 minutes), mechanical activity was suppressed using Blebbistatin[2] to prevent contraction. This process includes perfusing 200 ml of a concentrated 25 μM Blebbistatin solution and maintaining a modified Tyrode solution with 3 μM Blebbistatin throughout the experiment. To visualize electrical activity, the heart was stained with 1mg of voltage-sensitive dye (JPW-6003) through the heart's perfusion system.

The heart was positioned in the center of a custom-designed hexagonal acrylic tank (25 × 12 cm per face) filled with Tyrode solution maintained at 37°C through integrated heat exchangers. Thirty silver-coated copper electrodes (10 mm diameter) were distributed across two opposing faces of the tank to simulate electrodes placed on the left and right sides of a patient's torso. These electrodes were connected to an Intan RHD 64-channel acquisition system, recording at a 4 kHz sampling rate with 45.67 dB gain. An isolated needle inserted into the aortic root serves as the electrical mapping system's electrical reference.

For optical excitation of the voltage dye, six 650 nm LEDs illuminated the heart surface through a condenser lens and 650/40 nm bandpass filter. The resulting fluorescence was filtered through 700 nm long-pass filters and captured by two synchronized high-speed cameras (500 Hz) positioned to image the left and right ventricles at 540 × 720 pixel resolution. Hardware triggering was used to synchronize the optical and electrical recordings.

Electrical stimulation was delivered through a bipolar electrode positioned at the right ventricular base, applying pacing protocols with intervals ranging from 1000 to 200 ms or until 2:1 or arrhythmia is induced. This approach allowed assessment of both intrinsic conduction abnormalities and paced responses. The experimental design focused on correlating the high-resolution optical activation maps of the epicardial surface and the body surface potential measurements from the tank electrodes. Particular attention was given to how pathological conduction patterns in the explanted heart manifested in the non-invasive electrode recordings.

As this study represents the initial validation of the experimental platform, data were acquired from a single explanted heart obtained at VCU Medical Center under the approved IRB protocol. All protocols were designed to maximize the translational relevance, with the long-term goal of advancing clinically meaningful non-invasive mapping techniques.

2.3. Pre-processing

The optical signals underwent a structure processing pipeline to minimize baseline drift. A Butterworth high-pass filter with a cutoff frequency of 0.5 Hz was applied to suppress low-frequency fluctuations. To avoid signal distortion caused by frequency-dependent phase delays inherent to standard filtering methods, the MATLAB function 'filtfilt' is used. This function applies the filter in both forward and reverse directions, effectively canceling out any phase shifts to preserve the temporal alignment of signal components.

Subsequently, a spatiotemporal Gaussian smoothing filter was applied to further refine the signals. A spatial filter with 3×3 kernel was used to reduce signal spatial variance due to noise while enhancing local features. In parallel, a temporal filter with a kernel size of 5 was applied to smooth the signal over time, producing a more coherent temporal profile.

To align the optical signals with the electrical mapping signals used in later analyses, the optical mapping data is upsampled to 4 kHz using linear interpolation. This step ensured temporal synchronization between the optical and electrical signals with matching signal lengths.

The electrical signals underwent a series of filtering steps to enhance signal quality and suppress noise. First, a finite impulse response (FIR) band-pass filter was applied with a high-pass cutoff frequency of 0.5 Hz (order 5) and a low-pass cutoff frequency set at 250 Hz (order 10). To remove the 60 Hz line interference, a notch filter of order 6

was also applied. This combined filtering sequence yielded temporally and spatially coherent electrical signals, suitable for subsequent analysis and interpretation.

2.4. Wavefront propagation

The propagation of electrical wavefronts was characterized using both optical and electrical mapping techniques. For optical mapping, activation times were determined by analyzing the upstroke phase of optical action potentials (OAPs). A linear fitting approach (MATLAB's polyfit function) was applied to the OAP upstroke, with the activation time defined at the 50% rise point of the OAP signal (Fig. 1A). This method enabled the generation of high-resolution spatiotemporal maps of wavefront propagation across the epicardial surface.

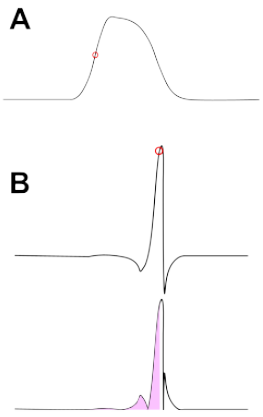

Figure 1. Activation Time Selection. A) The Optical mapping selection by 50% of the rise. B) The electrical activation selection, where the first image shows the signal and its selected point and the second one highlights the absolute of the signal with 50% of its area.

For electrical signal analysis, a center-of-mass (COM) approach was implemented to define activation points from non-invasive tank recordings. The COM was calculated as the time-point at which the area of absolute signal amplitude reached 50% of its total area during the activation window (Fig.1B). Mathematically, this is expressed as:

$$t_{\text{com}} = \min \left\{ t \mid \int_{t_0}^{t} |V(\tau)|\, d\tau \geq \frac{1}{2} \int_{t_0}^{t_1} |V(\tau)|\, d\tau \right\} \quad (1)$$

where $V(\tau)$ is the recorded potential, and $[t_0, t_1]$ denotes the analysis window. This method improved robustness against electric noise interference compared to traditional dV/dt-based approaches[3, 4].

3. Results

Figure 2 demonstrates the stability of wavefront propagation patterns across all tested pacing intervals (2000, 500, 400, 350, 300, and 1000 ms). Both optical (Fig. 2A) and electrical (Fig. 2B) maps show remarkably consistent activation sequences despite the progressive shortening and subsequent return to longer pacing intervals. Quantitative analysis revealed no significant correlation between local activation time distributions across pacing groups, indicating complete pacing rate independence.

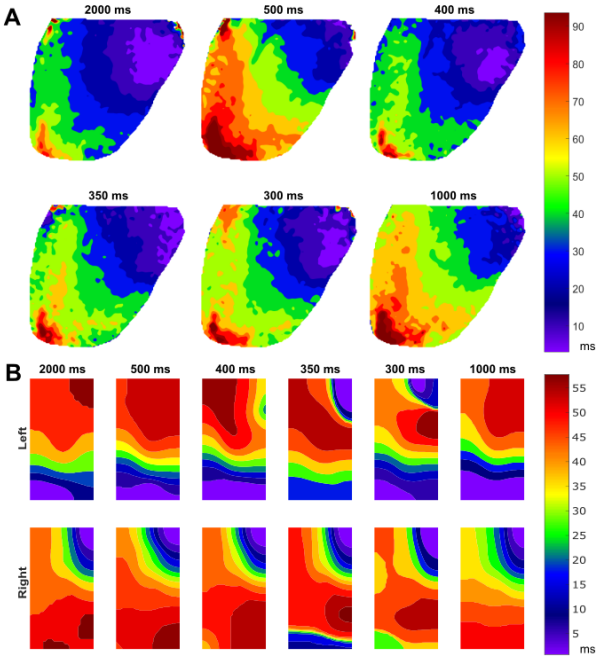

Figure 2. Wavefront propagation in different pacing stimulation intervals. A) The optical activation patterns for the left ventricle. B) the electrical activation pattern for the left and right faces of the tank.

The propagation in the right ventricle and across both tank faces did not change consistently with different pacing intervals. The preservation of activation patterns despite abrupt changes in cycle length suggests that the underlying electrophysiological pathology may have fundamentally impaired the tissue's ability to modulate conduction velocity[5].

In contrast, Figure 3 captures a spontaneous tachycardia episode that revealed fundamentally different propagation dynamics. Optical mapping (Fig. 3B) shows a distinct lateralized activation pattern, with wavefronts propagating from the anterior to posterior right ventricle - a complete departure from the uniform spread observed during pacing. The corresponding electrical maps (Fig. 3A) demonstrate how this conduction abnormality manifests differently on

the tank surface, showing the earliest activation in central electrodes rather than the characteristic vertical gradient seen in paced rhythms, highlighting the complex relationship between epicardial activity and surface potential patterns.

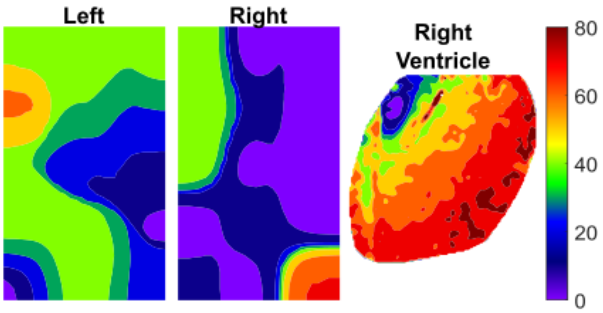

Figure 3. Wavefront propagation in a Tachycardia rhythm. A) shows the activation in the left and right tank surfaces. B) shows the epicardial activation in the surface of the heart by the right ventricle oriented camera.

The center-of-mass method proved particularly valuable for analyzing spontaneous events, reliably identifying activation times despite the complex signal morphology. A comparison between Figures 2B and 3B reveals that the two wavefront propagation maps exhibit distinct patterns of cardiac activation. This differentiation underscores the utility of our system in non-invasively identifying diverse activation patterns. By integrating both optical and electrical mapping techniques, we captured a more comprehensive representation of cardiac activity, offering insights that might be less discernible through single-modality approaches alone.

4. Conclusion

This experimental platform successfully maintains explanted human hearts in a viable condition for extended electrophysiological assessment, enabling both controlled pacing and autonomous activation studies. The platform's synchronized recordings revealed two key finding: (1) rate-independent conduction during increased pacing rates (Fig. 2), and (2) distinct propagation patterns during spontaneous tachycardia (Fig. 3), demonstrating that different conduction pathways can be characterized through non-invasive surface recordings.

Future enhancements will focus on increasing electrode density to better approximate existing FDA-approved BSPM systems (Medtronic) and implementing ECGi reconstruction. Machine learning approaches may leverage the system's unique paired optical-electrical datasets to improve non-invasive arrhythmia detection.

The observed dissociation between paced and spontaneous conduction patterns highlights the platform's potential for studying clinically relevant arrhythmia's mechanisms while preserving native human tissue properties, an essential advantage over animal models or simulations in translational electrophysiology research.

Acknowledgments

This work was supported in part by the São Paulo Research Foundation (FAPESP): T. Neves under grant #2024/02521-2; J.G.S. Paredes under grants #2020/03601-9 and #2023/04822-7 (BEPE); and J. Salinet under grant #2018/25606-2 and CNPq INCT INTERAS (call 58/2022). Additional support was provided by the Dr. Kenneth Ellenbogen Endowment. We thank the VCU surgeons for their support in providing explanted hearts for this study.

References

[1] Slater AD, Bartlett RH, Cohn JD, Griffith BP. Use of explanted human hearts as a model for the study of cardiac pathophysiologic conditions. The Journal of Thoracic and Cardiovascular Surgery 1995;110(1):196–200. DOI: 10.1016/s0022-5223(05)80030-3.

[2] Kovács M, Tóth J, Hetényi C, Málnási-Csizmadia A, Sellers JR. Mechanism of blebbistatin inhibition of myosin ii*. Journal of Biological Chemistry 2004;279(34):35557–35563. ISSN 0021-9258. DOI: https://doi.org/10.1074/jbc.M405319200.

[3] Dössel O, Krueger MW, Weber FM, Seemann G. Cardiac modelling for arrhythmia simulation and understanding. Computers in Biology and Medicine 2014;54:245–256. DOI: 10.1016/j.compbiomed.2015.04.027.

[4] Efimov IR, Nikolski VP, Salama G. Mapping cardiac arrhythmias: From molecular biology to the clinic. Journal of Cardiovascular Electrophysiology 2004;15(2):130–146. DOI:10.1111/j.1540-8167.2008.01356.x.

[5] Bramer D, Meier A, Schramm R, Müller-Edenborn B, Keller M, Arentz T, Jadidi AA, Dinov B. Influence of heart rate and change in wavefront direction through pacing on conduction velocity and voltage amplitude in a porcine model: A high-density mapping study. Journal of Personalized Medicine 2024;14(5):473. DOI: 10.3390/jpm14050473.

Address for correspondence:

Tainan Cerqueira Neves
Alameda da Universidade, S/N. Lab 107, Block Zeta.
Sao Bernardo do Campo - SP
Brazil
tainan.neves@ufabc.edu.br